Glibenclamide reverses cardiovascular abnormalities of Cantu syndrome driven by K_{ATP} channel overactivity

Conor McClenaghan,[1,2,3] Yan Huang,[1,2,3] Zihan Yan,[1,4] Theresa M. Harter,[1,2,3] Carmen M. Halabi,[1,5] Rod Chalk,[6] Attila Kovacs,[7] Gijs van Haaften,[8] Maria S. Remedi,[1,4] and Colin G. Nichols[1,2,3]

[1]Center for the Investigation of Membrane Excitability Diseases, [2]Department of Cell Biology, [3]Department of Physiology, [4]Division of Endocrinology, Department of Medicine, and [5]Division of Nephrology, Department of Pediatrics, Washington University School of Medicine, Saint Louis, Missouri, USA. [6]Structural Genomics Consortium, University of Oxford, Oxford, United Kingdom. [7]Department of Medicine, Washington University School of Medicine, Saint Louis, Missouri, USA. [8]Center for Molecular Medicine, Department of Genetics, University Medical Center Utrecht, Utrecht, Netherlands.

Cantu syndrome (CS) is a complex disorder caused by gain-of-function (GoF) mutations in *ABCC9* and *KCNJ8*, which encode the SUR2 and Kir6.1 subunits, respectively, of vascular smooth muscle (VSM) K_{ATP} channels. CS includes dilated vasculature, marked cardiac hypertrophy, and other cardiovascular abnormalities. There is currently no targeted therapy, and it is unknown whether cardiovascular features can be reversed once manifest. Using combined transgenic and pharmacological approaches in a knockin mouse model of CS, we have shown that reversal of vascular and cardiac phenotypes can be achieved by genetic downregulation of K_{ATP} channel activity specifically in VSM, and by chronic administration of the clinically used K_{ATP} channel inhibitor, glibenclamide. These findings demonstrate that VSM K_{ATP} channel GoF underlies CS cardiac enlargement and that CS-associated abnormalities are reversible, and provide evidence of in vivo efficacy of glibenclamide as a therapeutic agent in CS.

Introduction

Cantu syndrome (CS) is a complex disorder with multiple cardiovascular abnormalities, including edema, dilated and tortuous blood vessels with decreased systemic vascular resistance, patent ductus arteriosus (PDA), and marked cardiac hypertrophy (1). CS is caused by gain-of-function (GoF) mutations in *KCNJ8* and *ABCC9*, which encode pore-forming Kir6.1 and regulatory SUR2 subunits, respectively, of ATP-sensitive potassium (K_{ATP}) channels (2–12). These subunits are prominently expressed in smooth muscle (SM) cells, and vascular SM (VSM) K_{ATP} channel activation underlies the chronically dilated vasculature observed in patients with CS (13–17). Notably, Kir6.1 is not a major component of cardiomyocyte K_{ATP} channels (wherein the related Kir6.2 [*KCNJ11*] is the predominant pore-forming isoform [refs. 3, 18]) and so how CS-associated mutations in both *KCNJ8* and *ABCC9* result in cardiac hypertrophy is therefore unclear. We recently developed murine CS models in which disease-causing *ABCC9* or *KCNJ8* mutations were knocked-in to the equivalent mouse loci using CRISPR/Cas9. These animals exhibit increased VSM K_{ATP} channel activity and consequent chronic vasodilation, which we propose triggers systemic feedback mechanisms aimed at maintaining perfusion — including increased cardiac output and cardiomyocyte hypertrophy — in CS (19).

▶ Related Commentary: p. 1112

Conflict of interest: The authors have declared that no conflict of interest exists.

Submitted: May 24, 2019; **Accepted:** December 5, 2019; **Published:** February 17, 2020.
Reference information: *J Clin Invest*. 2020;130(3):1116–1121.
https://doi.org/10.1172/JCI130571.

There are currently no targeted therapies for CS and it is not known if, or to what extent, cardiovascular abnormalities can be reversed once manifest. K_{ATP} channel inhibitors, including the sulfonylurea glibenclamide (glyburide), are used clinically to treat diabetes due to their inhibitory action on pancreatic K_{ATP} channels (formed of Kir6.2/SUR1). These drugs also inhibit cardiovascular K_{ATP} channels and thus may potentially be repurposed for the treatment of CS (20). In this study we thus sought to directly test the hypothesis that cardiac hypertrophy occurs secondary to K_{ATP} GoF in VSM, to investigate whether cardiac remodeling in CS is reversible, and to test the potential for glibenclamide treatment of cardiovascular abnormalities in Cantu mice.

Results and Discussion

Cardiovascular abnormalities in CS result from K_{ATP} channel GoF in VSM cells. To directly test whether cardiac remodeling occurs as a secondary response to VSM K_{ATP} channel GoF, we crossed CS ($SUR2^{wt/AV}$) mice with animals expressing smooth muscle myosin heavy chain promoter-driven Cre-recombinase (SM-Cre) and dominant-negative *KCNJ8* (Kir6.1-AAA) transgenes, allowing inducible suppression of K_{ATP} in smooth muscle of WT and CS mice (Figure 1A). Induction of expression at 8 weeks resulted in complete loss of K_{ATP} function, determined by whole-cell patch clamp recordings from isolated aortic myocytes (Figure 1, B and C). As previously reported (19), $SUR2^{wt/AV}$ mice exhibit lower mean arterial pressure (MAP) than WT, and dominant-negative suppression of smooth muscle K_{ATP} on this CS background (in $SM\text{-}DN^{wt/AV}$ mice) resulted in significant MAP elevation (Figure 1, D and E). Most strikingly, cardiac hypertrophy was essentially completely reversed in $SM\text{-}DN^{wt/AV}$ mice 4 weeks after transgene induction (Figure 1F). These findings confirm a principal role for

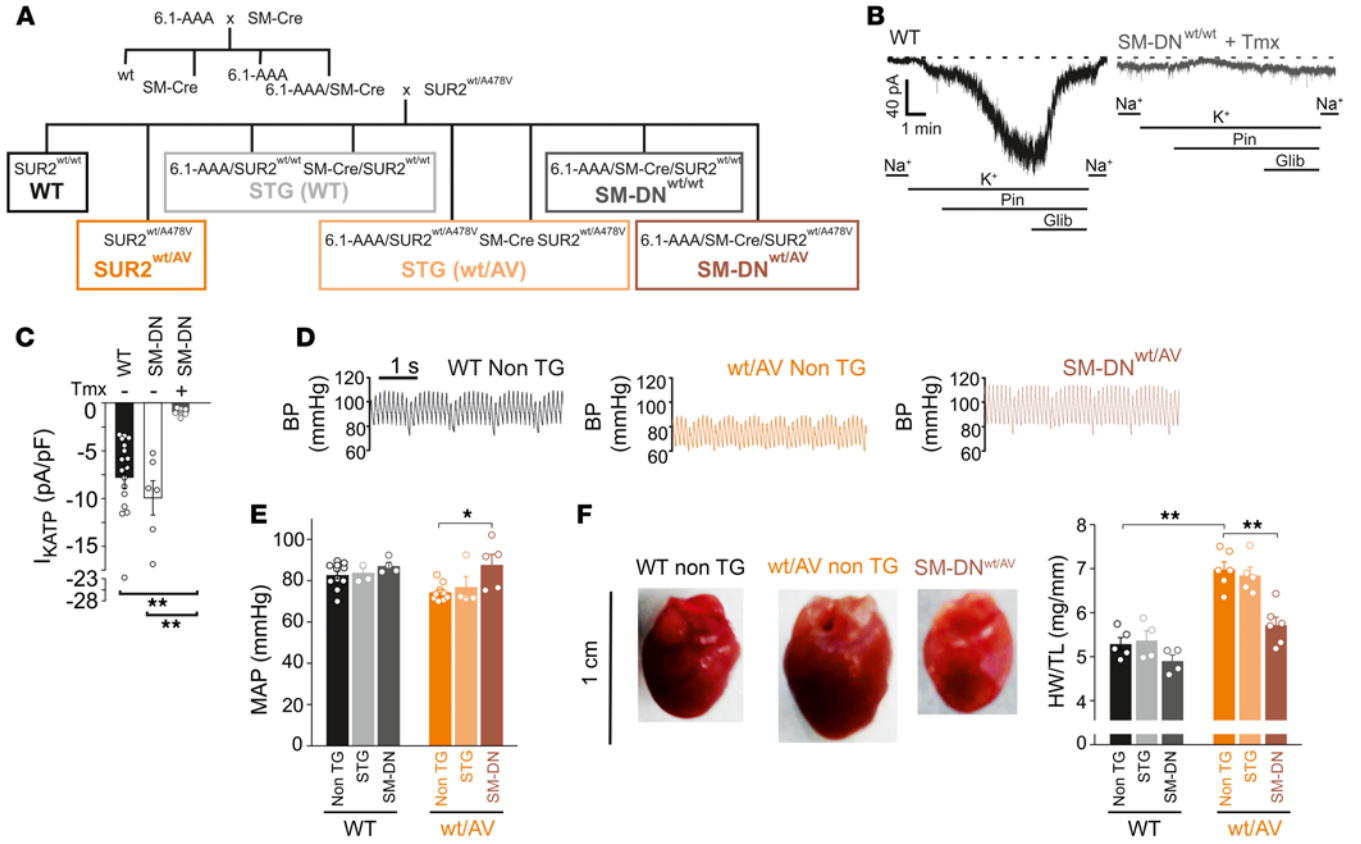

Figure 1. Downregulation of VSM K_{ATP} overactivity abolishes cardiac hypertrophy. (**A**) Transgenic approach to generate inducible, tissue-specific, dominant-negative Cantu mice (see text). (**B**) Representative whole-cell recordings of K_{ATP} channel activity in aortic SM cells from WT (left) and SM-DN$^{wt/wt}$ mouse following tamoxifen induction (right). Cells were voltage-clamped at –70 mV and currents recorded in high-Na^+ or -K^+ as indicated. Pinacidil (Pin) and glibenclamide (Glib) were administrated as indicated. (**C**) K_{ATP} channel current density from experiments as in **C**. Data for VSM cells isolated from WT (black bar), SM-DN$^{wt/wt}$ without tamoxifen induction (white bar), and SM-DN$^{wt/wt}$ with tamoxifen administration (gray bar). (**D**) BP recordings from anesthetized WT (black), SUR2$^{wt/AV}$ (orange), and SM-DN$^{wt/AV}$ (brown) mice. (**E**) Mean arterial pressure (MAP) in nontransgenic (Non TG), single-transgenic (STG), and double-transgenic (SM-DN) WT and SUR2$^{wt/AV}$ mice. (**F**) Left: Representative images of excised hearts from WT (top), SUR2$^{wt/AV}$ (middle), and SM-DN$^{wt/AV}$ (bottom) mice. Right: Heart size (heart weight normalized to tibia length; HW/TL) from nontransgenic (Non TG), single-transgenic (STG), and double-transgenic (SM-DN), WT and SUR2$^{wt/AV}$ mice. For all figures, individual data points are represented as open circles, bars show mean ± SEM. Statistical significance was determined by 1-way ANOVA and post hoc Tukey's test for pairwise comparison. *$P < 0.05$; **$P < 0.01$ from pairwise post hoc Tukey's test.

VSM K_{ATP} overactivity in the generation of cardiac hypertrophy. Importantly, they also show that cardiac hypertrophy can be reversed once manifest, and hence establish VSM K_{ATP} channels as appropriate molecular targets for pharmacological treatment of CS cardiovascular abnormalities.

Pharmacological reversal of CS-associated cardiovascular abnormalities in Cantu mice. We next hypothesized that reversal might also be achieved by pharmacological inhibition of overactive VSM K_{ATP} channels. Mice were implanted with subcutaneous, slow-release pellets formulated to release a moderate or high dose (approximately 1 or approximately 19 mg/kg/day) of glibenclamide for 4 weeks, which resulted in measured plasma concentrations of 30 ± 8 ng/mL (approximately 60 nM) and 147 ± 51 ng/mL (approximately 300 nM), respectively. Cardiac hypertrophy was reversed in a dose-dependent manner (Figure 2A), almost completely at the highest dose, comparable to the effect of genetically induced VSM K_{ATP} downregulation in SM-DN$^{wt/AV}$ mice (Figure 1). Consistent with an action on VSM K_{ATP} channels, high-dose glibenclamide elevated arterial pressure (MAP) and fully restored vascular resistance (SVR) in SUR2$^{wt/AV}$ mice (Figure 2, B and C). Glibenclamide also induced a partial reversal of the elevated cardiac index observed in SUR2$^{wt/AV}$ mice (Figure 2D). Hypertrophy in SUR2$^{wt/AV}$ mice is not associated with significant fibrosis, and fibrosis was not induced by glibenclamide (Figure 2E). Glibenclamide induced no impairment of cardiac function as determined by echocardiographic measurements of ejection fraction (Figure 2F).

Notably, high-dose glibenclamide did not reverse the marked carotid diameter enlargement observed in SUR2$^{wt/AV}$ mice (Figure 2G and ref. 19), and a similar resistance to reversal was observed in SMDN$^{wt/AV}$ mice (Figure 2H). This suggests that vascular structural abnormalities may be relatively refractory to K_{ATP} inhibition, but that reversal of conduit vessel structural remodeling is not required to reverse cardiac remodeling.

High-dose glibenclamide induces only transient hypoglycemia in mice. Glibenclamide is used clinically to treat diabetes, due to its inhibitory action on pancreatic Kir6.2/SUR1-dependent K_{ATP} channels (which exhibit markedly higher sensitivity than cardiovascular Kir6.1/SUR2 channels) (20). High doses, as required to reverse CS

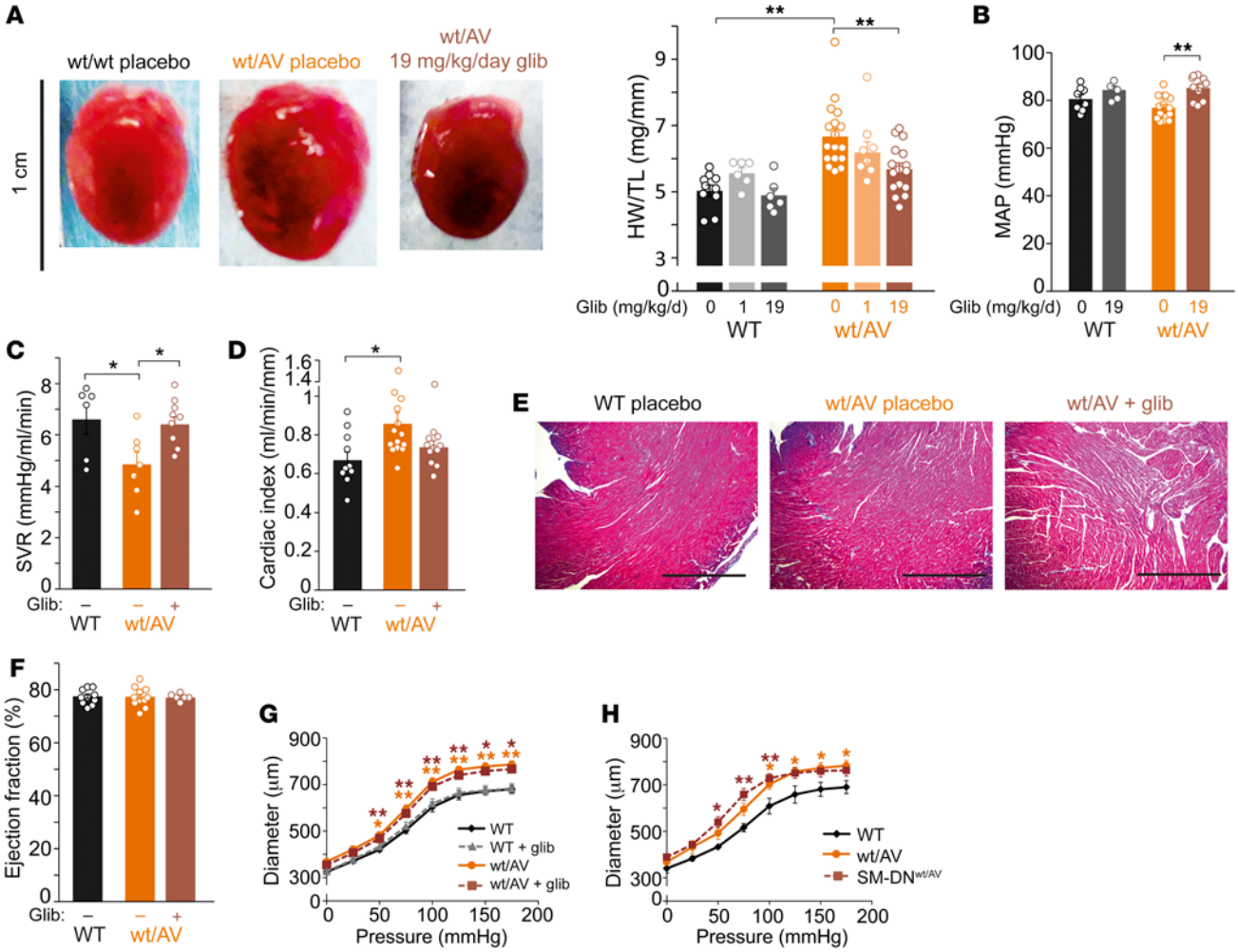

Figure 2. Glibenclamide reverses cardiac hypertrophy in SUR2$^{wt/AV}$ mice. (**A**) Left: Representative hearts from placebo-implanted WT (black), placebo-implanted SUR2$^{wt/AV}$ (orange), and approximately 19 mg/kg/day glibenclamide pellet implanted SUR2$^{wt/AV}$ (brown) mice. Right: Summary of heart size (weight normalized to tibia length; HW/TL) for WT and SUR2$^{wt/AV}$ mice implanted with either placebo pellets (Glib = 0), or pellets releasing approximately 1 mg/kg/day and approximately 19 mg/kg/day. (**B**) Summary of MAP in anesthetized placebo-pellet (Glib = 0) and approximately 19 mg/kg/day glibenclamide pellet–implanted WT and SUR2$^{wt/AV}$ mice. In all experiments, pellets were implanted at 8 weeks of age, and phenotypes were assessed 4 weeks later. (**C**) Systemic vascular resistance (SVR) and (**D**) cardiac index in placebo-implanted WT mice and placebo- or glibenclamide pellet–implanted SUR2$^{wt/AV}$ mice. (**E**) Gomori-stained left ventricular free wall sections. Scale bars: 500 μm. (**F**) Ejection fraction of placebo-implanted WT mice and placebo- or glibenclamide pellet–implanted SUR2$^{wt/AV}$ mice. Carotid artery compliance measurements from (**G**) placebo-implanted or approximately 19 mg/kg/day glibenclamide pellet–implanted WT and SUR2$^{wt/AV}$ mice, or (**H**) WT, SUR2$^{wt/AV}$, and SMDN$^{wt/AV}$ mice. Individual data points are represented as open circles, bars show mean ± SEM. Statistical significance was determined by 1-way ANOVA (**A**–**F**) and 2-way ANOVA (**G** and **H**) with subsequent post hoc Tukey's test for pairwise comparison. *$P < 0.05$; **$P < 0.01$ from pairwise post hoc Tukey's test. For **G** and **H**, color-coded statistical significance indicators are shown for comparison with placebo-implanted WT mice (black).

cardiovascular remodeling, will therefore also unavoidably inhibit pancreatic K_{ATP} channels and are thus naively predicted to increase insulin secretion and lower blood glucose (BG), a potentially important side effect that could limit clinical utility. As expected, fed BG was not different between WT and SUR2$^{wt/AV}$ mice prior to pellet implantation (Figure 3A) and both low- and high-dose glibenclamide indeed significantly lowered BG on day 1 after implantation. However, BG returned to normal by approximately day 2 (Figure 3, B–E). Moreover, fasted BG was normal in mice that had received high-dose glibenclamide for over 30 days — evidence of long-term glycemic stability (Figure 3F). Transient, spontaneously resolving, hypoglycemic effects of chronic glibenclamide have been demonstrated before, and are explained by chronic down-regulation of insulin secretion with continued K_{ATP}-inhibition (21). Consistent with this, a mild glucose intolerance phenotype was observed in high-dose–treated WT and SUR2$^{wt/AV}$ mice (Figure 3, G and H). Notably, in a single human CS case thus far treated with glibenclamide, transient hypoglycemia only was also observed at initiation of glibenclamide treatment or dose escalation (22), and thus chronic hypoglycemia may not prove to be a significant complication for glibenclamide therapy in patients with CS.

Glibenclamide-induced correction of low blood pressure in Kir6.1$^{wt/VM}$ mutant mice. Although the vast majority of patients with CS carry mutations in *ABCC9* (SUR2), there are patients with mutations in the pore-forming Kir6.1 (*KCNJ8*) subunit. To examine the potential for glibenclamide therapy in such patients, we also

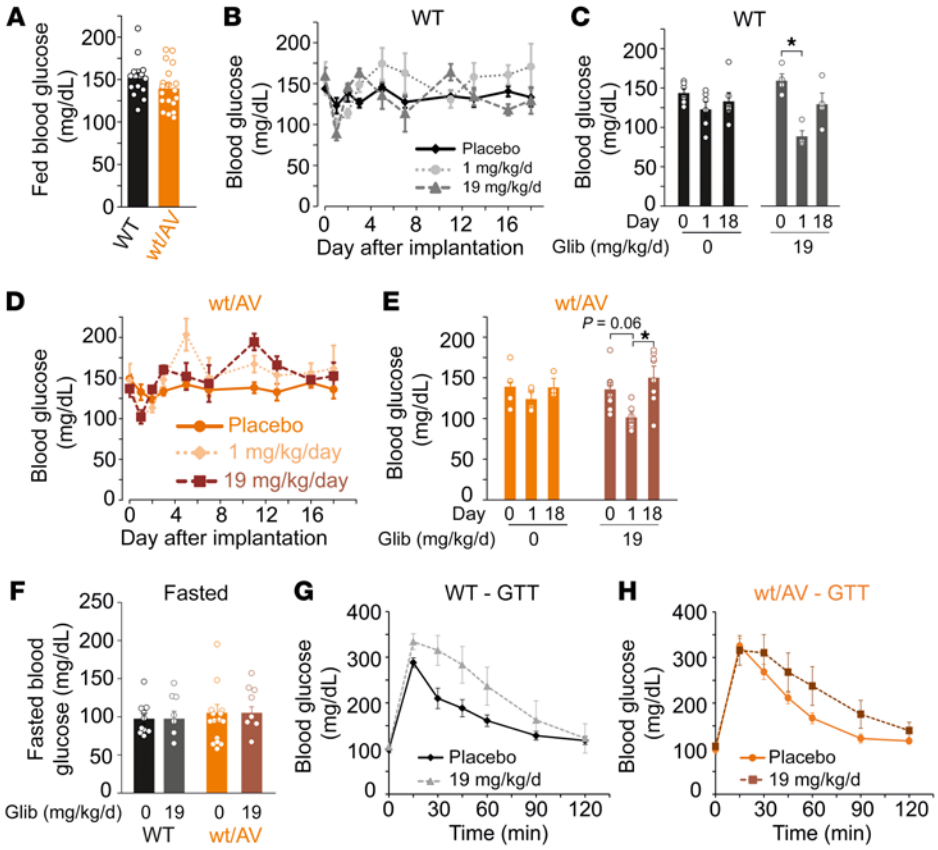

Figure 3. Chronic high-dose glibenclamide induces only transient hypoglycemia. (**A**) Summary of blood glucose levels in fed WT and SUR2$^{wt/AV}$ mice on day 0 prior to pellet implantation. (**B**) Mean blood glucose measurements from WT mice implanted with placebo pellets (black diamonds, solid line; n = 6), approximately 1 mg/kg/day glibenclamide pellets (light gray circles, dotted line; n = 4), and approximately 19 mg/kg/day glibenclamide pellets (dark gray triangles, dashed line; n = 4). (**C**) Summary of blood glucose measurements for WT mice implanted with placebo pellets (black bars) or approximately 19 mg/kg/day glibenclamide pellets (gray bars) on day 0, 1, and 18. (**D**) Mean blood glucose measurements from SUR2$^{wt/AV}$ mice implanted with placebo pellets (dark orange circles, solid line; n = 4), approximately 1 mg/kg/day glibenclamide pellets (light orange diamonds, dotted line; n = 7), and approximately 19 mg/kg/day glibenclamide pellets (brown squares, dashed line; n = 8). (**E**) Summary of blood glucose measurements for SUR2$^{wt/AV}$ mice implanted with placebo pellets (orange bars) or approximately 19 mg/kg/day glibenclamide pellets (brown bars) on day 0, 1, and 18. (**F**) Fasted BG in mice which had been implanted with either placebo or high-dose glibenclamide more than 30 days prior. Glucose tolerance test data for WT (**G**) and SUR2$^{wt/AV}$ (**H**) mice implanted with placebo or approximately 19 mg/kg/day glibenclamide pellets. For summary figures, individual data points are represented as open circles, bars show mean ± SEM. Statistical significance was determined by 1-way ANOVA and subsequent post hoc Tukey's test for pairwise comparison. *P < 0.05 from pairwise post hoc Tukey's test.

implanted CS model Kir6.1[V65M] knockin mice (Kir6.1$^{wt/VM}$) (19) with high-dose glibenclamide pellets. This resulted in a significant although incomplete (approximately 13 mmHg) improvement of the otherwise severe hypotensive phenotype and an incomplete effect on heart size (Figure 4, A and B). The Kir6.1[V65M] mutation results in a drastic GoF of K_{ATP} channels and causes severe CS features in humans (7, 8, 19). Unlike the SUR2[A478V] mutation, which does not significantly affect glibenclamide sensitivity (23), the Kir6.1[V65M] mutation markedly decreases glibenclamide inhibition in recombinant channels (8), potentially explaining the incomplete reversal of CV abnormalities. Alternatively, incomplete reversal might reflect the more severe phenotype requiring longer administration times for reversal. In either case, the reduced efficacy of glibenclamide in Kir6.1$^{wt/VM}$, compared with SUR2$^{wt/AV}$, suggests that sulfonylurea treatment efficacy may depend on the severity of the underlying mutation, and underlines the importance of thorough understanding of the molecular consequences for personalized therapy.

Inhibition of VSM K_{ATP} channels as a strategy to treat CS. The above results establish that cardiac remodeling in CS arises secondary to K_{ATP} channel GoF in VSM, and provide key preclinical evidence for in vivo efficacy of glibenclamide in treatment of CS. The link between VSM K_{ATP} channel GoF and cardiac hypertrophy is not yet established, but is likely to involve systemic feedback mechanisms that seek to normalize systemic perfusion in response to vasodilation. Directly inhibiting VSM K_{ATP} overactivity with K_{ATP} inhibitors may thus reverse both the primary vascular defect and these secondary features.

Excessive hair growth (hypertrichosis) is a defining CS feature (1), and is also mimicked by the K_{ATP} channel opener, minoxidil, which is used as a topical treatment for alopecia (24, 25). It is possible that K_{ATP} inhibition might alleviate hypertrichosis in patients with CS, and that topical administration of K_{ATP} inhibitors may be of cosmetic use for hair removal in the future (26). PDA is observed in most patients with CS and likely arises from the vasodilatory effect of excessive K_{ATP} activity in the DA after birth. PDA, which can be lethal without correction, is also present in approximately 1:2000 full-term births but in 20%–60% of premature births (27). K_{ATP} inhibitors may thus also prove useful for correction of PDA of various etiologies, an application that should be the subject of future study. Increased VSM K_{ATP} channel expression has been reported in septic shock, and previous animal studies suggested that K_{ATP} inhibition may also prove beneficial in treating endotoxic hypotension (28, 29), although acute glibenclamide treatment failed to reverse hypotensive shock in humans, despite inducing hypoglycemia (30, 31). Such studies illustrate the different sensitivity of pancreatic and cardiovascular K_{ATP} channels, and raise the question whether longer term and higher dose treatment might be necessary and appropriate for cardiovascular applications.

Potential adverse effects of high-dose glibenclamide, including actions in skeletal and cardiac muscle, as well as the drug

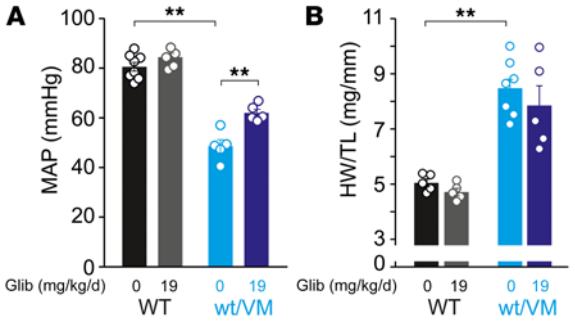

Figure 4. Partial reversal of cardiovascular features by glibenclamide in Kir6.1$^{wt/VM}$ mice. (**A**) Summary of mean arterial pressure (MAP) in anesthetized placebo-implanted (Glib = 0) and approximately 19 mg/kg/day glibenclamide pellet–implanted WT and Kir6.1$^{wt/VM}$ mice. (**B**) Summary of heart size (weight normalized to tibia length; HW/TL) for WT and Kir6.1$^{wt/VM}$ mice implanted with either placebo pellets (Glib = 0) or pellets releasing approximately 19 mg/kg/day. For all figures, individual data points are represented as open circles, bars show mean ± SEM. Statistical significance was determined by 1-way ANOVA and post hoc Tukey's test for pairwise comparison. $^{**}P < 0.01$ from pairwise post hoc Tukey's test.

sensitivity of specific CS mutations, require further study, and ideal therapy for CS may ultimately require an agent with much improved selectivity or potency for VSM Kir6.1/SUR2B channels. However, there is immediate need for a targeted therapy for CS, and the present findings clearly demonstrate the in vivo potential of glibenclamide for correcting CS cardiovascular abnormalities. Moreover, they suggest that the undesired glucose-lowering effects in nondiabetic animals are temporary, and may not therefore be prohibitive for the use of glibenclamide as a therapy in CS.

Methods

Mouse models. CRISPR/Cas9 genome-edited SUR2$^{wt/AV}$ and Kir6.1$^{wt/VM}$ Cantu mice were previously reported (19) (see also Supplemental Methods; supplemental material available online with this article; https://doi.org/10.1172/JCI130571DS1). Dominant-negative Kir6.1-AAA mice were crossed with Cantu mice as illustrated in Figure 1A and described in detail in Supplemental Methods. Electrophysiological recordings of acutely isolated aortic smooth muscle cells, blood pressure measurements in anesthetized mice, echocardiographic analysis and heart weight measurements, Gomori stain, vascular compliance, and blood glucose measurements were made as described in Supplemental Methods. Plasma glibenclamide concentrations were measured by LC-MS/MS analysis using an ion trap mass spectrometer following the method described in detail in Supplemental Methods.

Study approval. Mouse studies were performed in compliance with the standards for the care and use of animal subjects defined in the NIH Guide for the Care and Use of Laboratory Animals and were reviewed and approved by the Washington University Institutional Animal Care and Use Committee.

Statistics. Statistical analysis was carried out with Microsoft Excel (Real Statistics Resource Pack software, www.real-statistics.com). Significance values were calculated using 1-way ANOVA and subsequent post hoc Tukey's test for pairwise comparison. For carotid compliance measurements, where groups with 2 variables were compared, 2-way ANOVA with post hoc Tukey's test was performed using GraphPad Prism 8 for OS X. A P value of less than 0.05 was considered significant. All values are expressed as mean ± SEM.

Author contributions

CM and CGN designed research studies. CM, YH, ZY, CMH, RC, TMH, and AK conducted experiments and acquired and analyzed data. CM and CGN wrote the manuscript. GVH and MSR provided advice. All authors critically reviewed the manuscript.

Acknowledgments

This work was supported by NIH R35 HL140024 (to CGN). CM was supported by American Heart Association Postdoctoral Fellowship 19POST34380407. CMH was supported by NIH K08 HL135400 and Pilot and Feasibility grant CIMED-18-04. The Kir6.1-AAA mice were provided by William A. Coetzee (New York University, New York, New York).

Address correspondence to: Colin G. Nichols, Box 8228, Washington University School of Medicine, 660 South Euclid Avenue, Saint Louis, Missouri 63110, USA. Email: cnichols@wustl.edu.

YH's present address is: Department of Cardiology, Renmin Hospital of Wuhan University, Wuhan, China.

1. Grange DK, Nichols CG, Singh GK. Cantu syndrome and related disorders. In: Adam MP, et al, eds. *GeneReviews*. Seattle, Washington, USA: University of Washington; 2014.
2. Nichols CG. KATP channels as molecular sensors of cellular metabolism. *Nature*. 2006;440(7083):470–476.
3. Foster MN, Coetzee WA. KATP channels in the cardiovascular system. *Physiol Rev*. 2016;96(1):177–252.
4. Harakalova M, et al. Dominant missense mutations in ABCC9 cause Cantú syndrome. *Nat Genet*. 2012;44(7):793–796.
5. van Bon BW, et al. Cantú syndrome is caused by mutations in ABCC9. *Am J Hum Genet*. 2012;90(6):1094–1101.
6. Cooper PE, et al. Cantú syndrome resulting from activating mutation in the KCNJ8 gene. *Hum Mutat*. 2014;35(7):809–813.
7. Brownstein CA, et al. Mutation of KCNJ8 in a patient with Cantú syndrome with unique vascular abnormalities - support for the role of K(ATP) channels in this condition. *Eur J Med Genet*. 2013;56(12):678–682.
8. Cooper PE, McClenaghan C, Chen X, Stary-Weinzinger A, Nichols CG. Conserved functional consequences of disease-associated mutations in the slide helix of Kir6.1 and Kir6.2 subunits of the ATP-sensitive potassium channel. *J Biol Chem*. 2017;292(42):17387–17398.
9. Isomoto S, et al. A novel sulfonylurea receptor forms with BIR (Kir6.2) a smooth muscle type ATP-sensitive K+ channel. *J Biol Chem*. 1996;271(40):24321–24324.
10. Inagaki N, et al. Cloning and functional characterization of a novel ATP-sensitive potassium channel ubiquitously expressed in rat tissues, including pancreatic islets, pituitary, skeletal muscle, and heart. *J Biol Chem*. 1995;270(11):5691–5694.
11. Chutkow WA, Simon MC, Le Beau MM, Burant CF. Cloning, tissue expression, and chromosomal localization of SUR2, the putative drug-binding subunit of cardiac, skeletal muscle, and vascular KATP channels. *Diabetes*. 1996;45(10):1439–1445.
12. Tessadori F, et al. Effective CRISPR/Cas9-based nucleotide editing in zebrafish to model human genetic cardiovascular disorders. *Dis Model Mech*. 2018;11(10):dmm035469.
13. Quayle JM, Standen NB. KATP channels in vascular smooth muscle. *Cardiovasc Res*. 1994;28(6):797–804.
14. Aziz Q, et al. The ATP-sensitive potassium channel subunit, Kir6.1, in vascular smooth muscle

plays a major role in blood pressure control. *Hypertension*. 2014;64(3):523–529.
15. Li A, et al. Hypotension due to Kir6.1 gain-of-function in vascular smooth muscle. *J Am Heart Assoc*. 2013;2(4):e000365.
16. Chutkow WA, et al. Episodic coronary artery vasospasm and hypertension develop in the absence of Sur2 K(ATP) channels. *J Clin Invest*. 2002;110(2):203–208.
17. Miki T, et al. Mouse model of Prinzmetal angina by disruption of the inward rectifier Kir6.1. *Nat Med*. 2002;8(5):466–472.
18. Flagg TP, Enkvetchakul D, Koster JC, Nichols CG. Muscle KATP channels: recent insights to energy sensing and myoprotection. *Physiol Rev*. 2010;90(3):799–829.
19. Huang Y, et al. Cardiovascular consequences of KATP overactivity in Cantu syndrome. *JCI Insight*. 2018;3(15):e121153.
20. Gribble FM, Tucker SJ, Seino S, Ashcroft FM. Tissue specificity of sulfonylureas: studies on cloned cardiac and beta-cell K(ATP) channels. *Diabetes*. 1998;47(9):1412–1418.
21. Remedi MS, Nichols CG. Chronic antidiabetic sulfonylureas in vivo: reversible effects on mouse pancreatic beta-cells. *PLoS Med*. 2008;5(10):e206.
22. Ma A, et al. Glibenclamide treatment in a Cantú syndrome patient with a pathogenic ABCC9 gain-of-function variant: Initial experience. *Am J Med Genet A*. 2019;179(8):1585–1590.
23. Cooper PE, Sala-Rabanal M, Lee SJ, Nichols CG. Differential mechanisms of Cantú syndrome-associated gain of function mutations in the ABCC9 (SUR2) subunit of the KATP channel. *J Gen Physiol*. 2015;146(6):527–540.
24. Fenton DA, Wilkinson JD. Topical minoxidil in the treatment of alopecia areata. *Br Med J (Clin Res Ed)*. 1983;287(6398):1015–1017.
25. Fiedler-Weiss VC. Topical minoxidil solution (1% and 5%) in the treatment of alopecia areata. *J Am Acad Dermatol*. 1987;16(3 Pt 2):745–748.
26. Newfield RS. Topical sulfonylurea as a novel therapy for hypertrichosis secondary to diazoxide, and potentially for other conditions with excess hair growth. *Med Hypotheses*. 2015;85(6):969–971.
27. Shelton EL, Singh GK, Nichols CG. Novel drug targets for ductus arteriosus manipulation: Looking beyond prostaglandins. *Semin Perinatol*. 2018;42(4):221–227.
28. Landry DW, Oliver JA. The ATP-sensitive K+ channel mediates hypotension in endotoxemia and hypoxic lactic acidosis in dog. *J Clin Invest*. 1992;89(6):2071–2074.
29. Vanelli G, Hussain SN, Aguggini G. Glibenclamide, a blocker of ATP-sensitive potassium channels, reverses endotoxin-induced hypotension in pig. *Exp Physiol*. 1995;80(1):167–170.
30. Warrillow S, Egi M, Bellomo R. Randomized, double-blind, placebo-controlled crossover pilot study of a potassium channel blocker in patients with septic shock. *Crit Care Med*. 2006;34(4):980–985.
31. Morelli A, et al. Glibenclamide dose response in patients with septic shock: effects on norepinephrine requirements, cardiopulmonary performance, and global oxygen transport. *Shock*. 2007;28(5):530–535.